Erosive Intensity Measurements of Cavitating Jet with Various Configurations

H. Kato and Y. Shimomura
Department of Mechanical Engineering
Toyo University
Kujirai 2100, Kawagoe, 350-8585 JAPAN
Fax: +492-33-9779, E-mail: kato@eng.toyo.ac.jp

Abstract

Cavitating jets are widely used for cleaning, cutting, improving material strength and so forth. This paper describes the erosive intensity measurement of a cavitating jet with various nozzle configurations. Two cross-shaped nozzles, one circular nozzle with two cross wires, and two nozzles with swirl vanes, were tested. The authors expected an increase of erosive intensity to come about by the use of these nozzles, as a result of the deformation of the vortex ring in the cavitating jet. However, the experimental results reveal a decrease of erosive intensity contrary to expectations.

Key words: cavitating jet, cavitation, noncircular nozzle, erosion,

1. Introduction

Cavitation is perceived negatively by designers of screw propellers and fluid machinery. This is because cavitation causes damage and noise. Nevertheless, it is widely used for cleaning, cutting, mixing, improving material strength, agitating chemical reactions, and so forth. Kato (2000) reviewed a wide variety of cavitation applications for practical purposes. The applications extended from the cleaning of a cylinder block of a car engine to the cutting of human kidney as a surgical knife. Among these applications, a cavitating jet is very commonly used for cleaning, cutting, digging and peening. A normal circular nozzle with a straight hole is common for the generation of a cavitating jet because of its simplicity (for example. Lichtarowicz (1981)). Although an increase of the jet flow velocity is the most direct way in which to increase the erosive intensity of a cavitating jet, various other methods have been proposed and tested. Terasaki et al. (1999) attached a cavitator in the nozzle of a cavitating jet, and reported that the erosive intensity of the cavitating jet increased three times. Shimizu et al. (1999) tested a square nozzle and found that the square cavitating jet produced a noncircular erosion pattern.

Jet flow is accompanied by vortex rings, which induce velocity and provide three-dimensional modification of the vortex ring, because the induced velocity is dependent on the strength and curvature of the vortex ring. A good example is smoke rings of a cigarette. With the noncircular jet flow, which may have a sharp angle, we can expect that intense three-dimensional modification of a vortex ring arises. Swirled jet flow has a longitudinal vortex at the center. Cavitation bubbles are generated in the low-pressure region of the vortex core. Therefore, the erosive intensity of these cavitating jets should be different to that of a normal circular cavitating jet. Erdmann-Jesnitzer et al. (1976) reported that the digging ability increased by adding swirl to a water jet flow.

Based on these findings, the nozzle shape was widely varied in this paper and we expected to observe an increase of the erosive intensity of the cavitating jet. The tested nozzles were two cross-shaped nozzles, one circular nozzle with two cross wires, and two nozzles with swirl vanes. A normal circular nozzle was also tested for comparison.

2. Experimental Method and Tested Nozzles

A schematic flow diagram of the experimental apparatus is shown in Fig. 1. The water in the water tank was pressurized to a maximum pressure of 15MPa using a plunger pump with three plungers, and was then blown off in a test chamber through a nozzle, forming a cavitating jet. The flow rate of the cavitating jet was adjusted by controlling the flow rate of the water, which passed along a bypass pipe via a valve. In order to prevent pulsation as a result of the plunger pump, an accumulator was attached to the middle of the pipeline. We measured pressures upstream of the nozzle and in the test chamber, and calculated the flow velocity and cavitation number from these measured values. In the measurement of pressure, two digital pressure gauges were used (Sokken PE-33-G, Measurement range: 15MPa and 1.5MPa, Accuracy: 0.3% of full scale) Two filters were attached to the middle of the flow pipeline, so that tiny eroded particles did not enter the plunger pump or the nozzle.

The test chamber is shown in Fig. 2. The cavitating jet, which is blown off from the nozzle, impinged the center of test piece vertically. The test piece was 10mm in diameter and 4mm thick, and was made from aluminum alloy. Table 1 shows the composition of the aluminum alloy. The Vickers hardness of the aluminum alloy was 85. The standoff distance between the nozzle and the test piece was an important test parameter and could be varied from 0 to 45mm. It is expressed in nondimensional form with the diameter of a nozzle in this paper.

The cavitation number of 0.02 was chosen from the preliminary experiment, because it was the most erosive condition. Initially, we intended to perform all the experiments with the same pressure difference between the upstream position and that in the test chamber. However, this was impossible because of large difference in pressure loss among nozzles. The upstream and downstream pressures were set to 11.7-11.9MPa and 0.23-0.24MPa for circular nozzles, respectively. The standard exposure time was 10 minutes. The water temperature was maintained at 25-30 degrees throughout the experiment. The experimental conditions are summarized in Table 2. The jet flow velocity ranged from 73.5-124.5m/s.

The amount of weight loss and the surface roughness increases of the test piece were measured to evaluate the erosive intensity in the preliminary experiment. Weight loss was measured using an electronic balance (Shimadzu AX-120, Minimum reading: 0.1mg). The surface roughness was measured using a roughness measuring apparatus (Mitutoyo Surftest, SV-402).

The tested nozzles are as follows.

(1) Two normal circular nozzles (0.4mm and 0.6mm in diameter).

(2) Two cross-shaped nozzles (Fig. 3 (a)). The lengths of the cross shape were 0.6mm and 0.8mm.

(3) A circular nozzle with two cross wires (0.15mm in diameter) (Fig. 3 (b)).

(4) Two nozzles with three swirl vanes on the upstream side (Fig. 4). The vane angles were 15 and 30 degrees. The diameters of the nozzles were 0.4mm and 0.6mm.

The normal circular nozzles of (1) were tested for comparison with other nozzles. The cross-shaped nozzles of (2) were selected by taking the three-dimensional modification of the ring vortex into consideration, as stated previously. The interference of four ring vortexes generated at the outlet of nozzle of (3) was aimed at, as shown in Fig. 5. In these jets, the axis of the vortexes was vertical to the direction of the cavitating jet. On the other hand, the nozzles with swirl vanes were aimed to generate a vortex with an axis that was parallel to the flow at the center of the cavitating jet.

3. Experimental Results and Considerations

3.1 Influence of Flow Velocity and Exposure Time

The influences of flow velocity and exposure time, which are important parameters in cavitation erosion, were investigated in the experiment. The nondimensional standoff distance was set at 25. In many previous papers, the weight loss rate or the mean depth of penetration rate (MDPR) is often used as a good measure of the erosive intensity. On the other hand, it is known that the roughness increase (R) is a good index in the early stage of erosion. (Kato (1975A, 1975B, 1976)) The roughness increase is easy to measure. Moreover, we can reduce the experimental time comparing to the weight loss measurement. Figures 6 and 7 show the increase in roughness, and the increase in eroded area to the flow velocity, respectively. Since the erosion is generated in the shape of a doughnut, we measured the inner and outer diameters of the eroded area visually and calculated the eroded area. The product of roughness and the eroded area is equivalent to the plastic deformation volume (PDV). The influence of the flow velocity on the PDV is shown in Fig. 8.

From Figs. 6 and 8 we can deduce the following relations;

$$R \propto V^{6.0}, \quad \text{and} \quad PDV \propto V^{8.4}.$$

Figure 9 shows the increase in mass loss and surface roughness to time. When the exposure time was long, the surface roughness becomes too large, and is difficult to measure using a conventional roughness measuring apparatus. The data shown in Fig. 9 were obtained from different test pieces for each exposure time, not a series of measurements on one test piece. Figure 10 shows photographs of eroded surface of these test pieces. The round shape of the eroded area collapses as time passes, although erosion occurs in the shape of a doughnut in the early stages of erosion. Although the scatter of the data for weight loss increases with time, these results reveal that the reproducibility in the present experiment is good.

3.2 Results of Cross-Shaped Nozzles and the Circular Nozzle with Two Cross Wires

Figure 11 shows the result of the two cross-shaped nozzles (Fig. 3 (a)) and the circular nozzle with two cross wires (Fig. 3 (b)). The experimental conditions are listed in Table 2. The erosive intensity of those nozzles of noncircular shape was much smaller than that of a normal circular nozzle, contrary to expectations. Observation of the cavitating jet from the circular nozzle with two cross wires revealed that the jet was divided by wires and that the spread angle of the jet became large. This seemed to be the reason why the erosive intensity was so low. The modification of the vortex ring did not lead to improvement in the erosive intensity of a cavitating jet.

3.3 Results of Nozzles with Swirl Vanes

The erosive intensity was measured for nozzles of swirl vanes. Two nozzles (0.4mm and 0.6mm in diameter) and two swirl vanes (15 degrees and 30 degrees) were combined, respectively. Therefore, four types of experiments were performed as shown in Figs. 12 and 13. All the experiments were carried out twice under the same conditions. The result of the normal circular nozzle is also shown for comparison. The erosive intensity of the nozzles with swirl vanes is weaker than that of a normal circular nozzle, particularly for those with swirl vanes of 30 degrees. Moreover, the pattern of eroded surface was doughnut-shaped and did not change with the introduction of a longitudinal vortex at the center of the cavitating jet (Fig. 5). Thus, we face to a dilemma; when we increase the angle of the swirl vanes to strengthen the longitudinal vortex, the jet velocity decreases because of the increase of drag.

4. Conclusions

The erosive intensity of cavitating jets was examined with nozzles that were not of normal circular shape. The tested nozzles were two cross-shaped nozzles, a circular nozzle with cross wires, and two nozzles with swirl vanes. The intention was to modify the vortex in the cavitating jet, in order to increase the erosive intensity and/or to change the erosion pattern. None of the nozzles could achieve the intended purpose. The erosive intensity became weaker and the doughnut-shaped eroded area did not change. Conversely, the present method employed in this experiment may be considered useful for weakening the erosion strength of a cavitating jet.

Acknowledgement

The authors thank very much the students, Messrs. T. Kurushima, T. Tanaka, and T. Kikuchi for their efforts during the experiment.

References

Erdmann-Jesnitzer. M. Hassan and H. Luis. （1976）: “A Study of the Oscillations Effects on the Cleaning and Cutting Efficiency of High Speed Water Jet,” Proc. 3rd International symposium on Jet Cutting Technology, BHRA, pp. C3-27-C3-41

Kato, H. (1975A): "A New Cavitation Erosion Test Method and its Application to a Ducted Propeller," International Shipbuilding Progress, Vol.22, No.253, pp. 291-304

Kato, H. (1975B): "A Consideration on Scaling Laws of Cavitation Erosion," International Shipbuilding Progress, Vol.22, No.253, pp. 305-327.

Kato, H. (1976): "On the Prediction Method of Cavitation Erosion from Model Test," Symp. Grenoble 1976, IAHR.

Kato, H. (2000): "Cavitation, The Unique Characteristics and Utilization," 4th Int. Conf. on Hydrodynamics (ICHD2000), Yokohama, pp. 85-95

Lichitarowicz, A. (1981): "Erosion Testing with Cavitating Jet," Cavitation Erosion in Fluid Systems, ASME, Fluids Engineering Conference, pp. 83-94

Shimizu, S. et al. (1999): "Flow Structures and Erosive Properties of Non-Circular Cavitating Jet," 10th Symposium on Cavitation, Fukui, Japan, pp. 75-78 (in Japanese)

Terasaki, N., Fujikawa, S., Takasugi, N., Hayama, S., and Sugino, Y. (1999): "Improvement of Machining Performance of Submerged Water Jet by Cavitator," Int. Symp. on New Application of Water Jet Technology, Ishinomaki, Japan, pp. 129-133

Table 1 Composition of aluminum alloy

Chemical component	Si	Fe	Cu	Mu	Mg	Cr	Zn	Al
%	0.04	0.10	0.00	0.06	4.8	0.06	0.00	Rest

Table 2 Experimental conditions

	Velocity (m/s)	Flow rate (ml/min)	Downstream Pressure(MPa)	Upstream Pressure(MPa)
Normal circular nozzle (0.6mm dia)	**124.0**	**2130**	**0.23**	**11.7**
Normal circular nozzle (0.4mm dia)	**118.0**	**900**	**0.23**	**11.9**
Cross-shaped nozzle (0.6mm dia)	**88.5**	**1380**	**0.23**	**11.8**
Cross-shaped nozzle (0.8mm dia)	**73.5**	**1750**	**0.19**	**9.5**
Circular nozzle with two wires	**90.5**	**2150**	**0.23**	**11.9**
Nozzle with swirl vanes (0.4mm dia+15, degree)	**115.0**	**875**	**0.24**	**11.9**
Nozzle with swirl vanes (0.6mm dia+15, degree)	**124.5**	**2100**	**0.24**	**11.9**

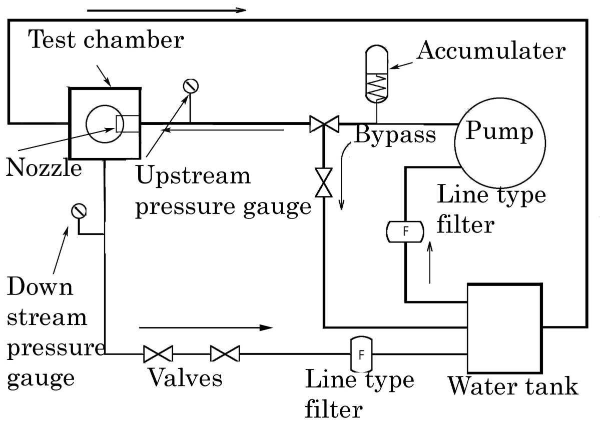

Figure 1 Schematic flow diagram of the experimental apparatus

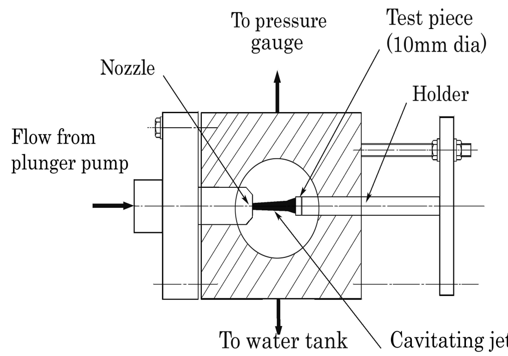

Figure 2 Test chamber

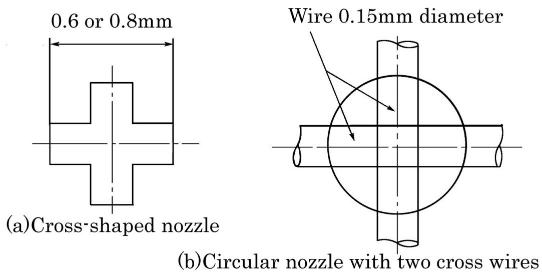

Figure 3 Cross-shaped nozzle and circular nozzle with two cross wires

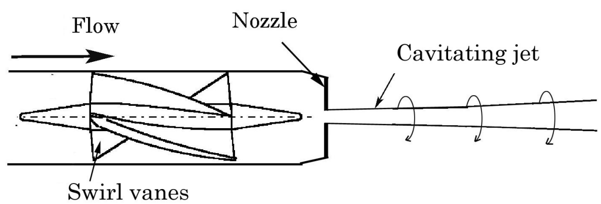

Figure 4 Nozzle with swirl vanes

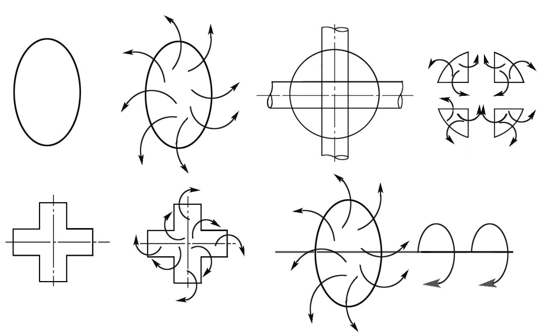

Figure 5 Three-dimensional modification of vortex in a jet flow

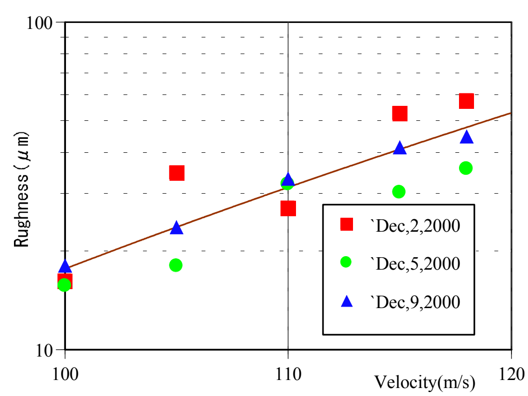

Figure 6 Surface roughness increase vs. flow velocity

(Exposuretime:10min,Non-dimensioal standoff distance:25)

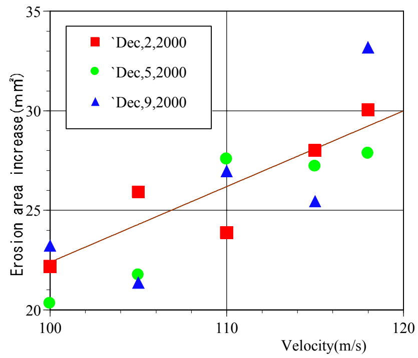

Figure 7 Erosion area increase vs. flow velocity (Exposuretime:10min, Non-dimensioal standoff distance:25)

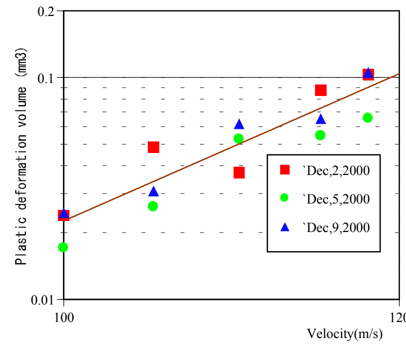

Figure 8 Influence of the flow velocity on plastic deformation volume (PDV) (Exposuretime:10min, Non-dimensioal standoff distance:25)

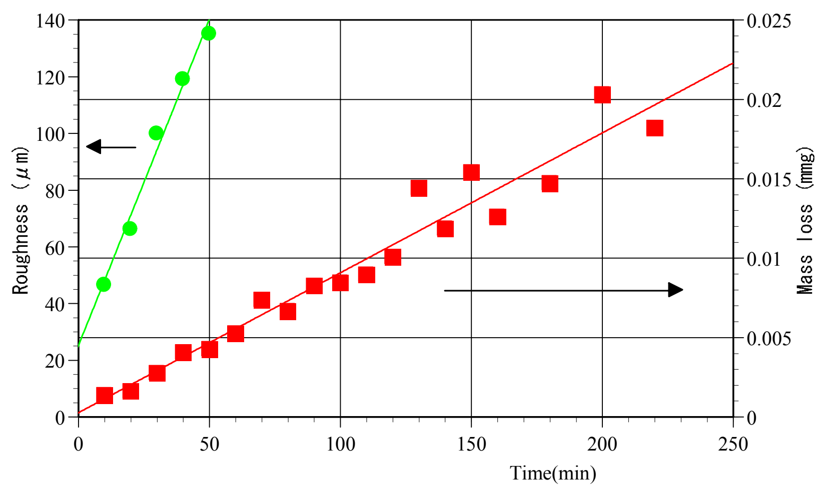

Figure 9 Mass loss and surface roughness

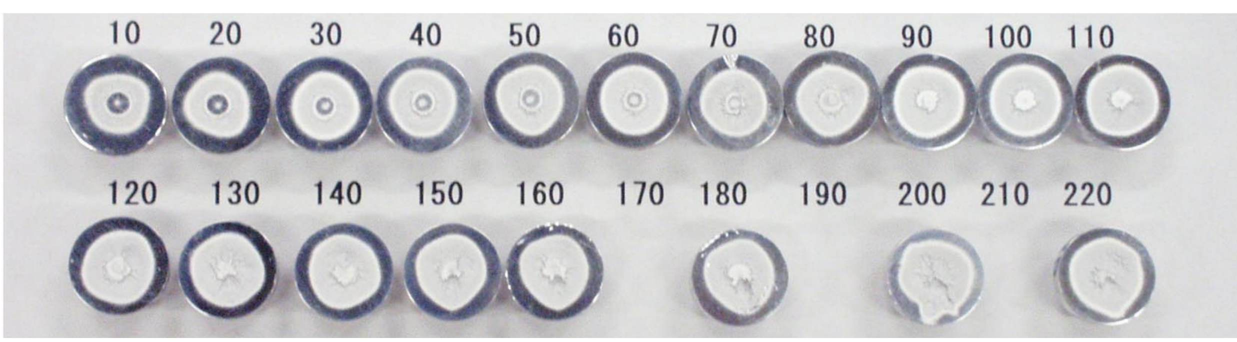

Figure 10 Appearance of eroded surface of test pieces with time (Number in the figure are exposure times in minutes)

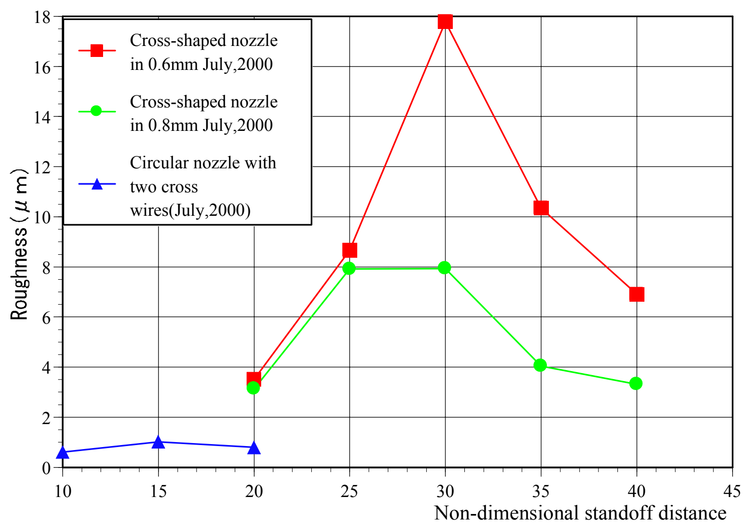

Figure 11 Comparison of erosive intensity increase of various nozzle configurations with time

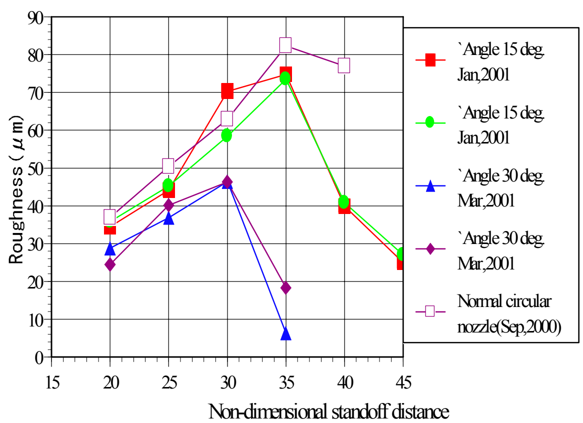

Figure 12 Erosive intensity of a nozzle with swirl vanes (diameter of nozzle: 0.4mm) (Exposure time: 10min)

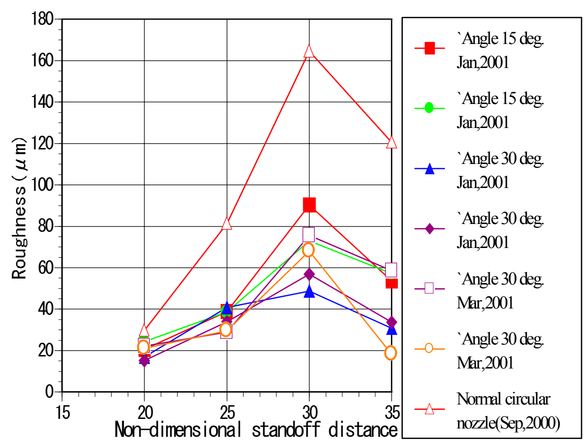

Figure 13 Erosive intensity of a nozzle with swirl vanes (diameter of nozzle: 0.6mm) (Exposure time: 10min)